RF-MBE GROWTH OF III-NITRIDES HETEROSTRUCTURES FOR LIGHT DETECTING APPLICATIONS

MOHD ZAKI BIN MOHD YUSOFF

UNIVERSITI SAINS MALAYSIA
2016

RF-MBE GROWTH OF III-NITRIDES HETEROSTRUCTURES FOR LIGHT DETECTING APPLICATIONS

by

MOHD ZAKI BIN MOHD YUSOFF

Thesis submitted in fulfillment of the requirements for the degree of Doctor of Philosophy

March 2016

ACKNOWLEDGEMENTS

All praises is due to Allah for His blessings and guidance. I would like to express my sincere gratitude to my main supervisor, Prof. Dr. Zainuriah Hassan, for her scientific guidance, valuable time and motivational support throughout the course of this study. I also would like to thank my both co-supervisors, Prof. Dr. Haslan Abu Hassan and Prof. Dr. Mat Johar Abdullah, for their valuable guidance, time and comments. Special thank goes to NOR laboratory staffs for their help and technical support offered during my research works, especially Ms Ee Bee Choo, Mr. Mohtar, Mr. Jamil, and Mr. Hazhar. Not forgotten are our research officers, Mr. Anas Ahmad, Mr. Yushamdan, and Ms Siti Khadijah Bakhori which provide me the technical support. I would like to express my thanks to MBE team especially Mr. Chin Che Woei, Dr. Sabah Thahab, Dr. Magdy and others for their assistance, guidance and technical support mainly in sample preparation and experimental set up during my research work. I would like to express my thanks to my friends as well as my research colleagues, Ms Ainorkhillah, Ms Rosfariza, Ms Azzafeerah, Dr. Chuah Lee Siang, Dr. Naser and many more, for their assistance in many aspects such as sample characterization and experimental set up. My gratitude goes to Kementerian Pendidikan Tinggi Malaysia for providing me the opportunity and financial resources. Last but not least, my deepest thanks go to my lovely wife, Ms Wan Najwa Haji Wan Ali, my children, Ahmad Nazhan Mohd Zaki, Afia Natasha Mohd Zaki, my parents, Mr. Mohd Yusoff Abd Hamid and Kamariah Haji Mamat, and my siblings for their love, encouragement, and support to me in completing my studies.

TABLE OF CONTENTS

CHAPTER 3: INSTRUMENTATION AND METHODOLOGY

LIST OF TABLES

LIST OF FIGURES

LIST OF SYMBOLS

α	Absorption coefficient
ε_o	Absolute dielectric constant
T	Absolute temperature
A	Area
E_g	Band gap
k	Boltzmann's constant
μ	Carrier mobility
I	Current
W_D	Depletion layer width
ε	Dielectric permittivity
d	Distance
m^*	Effective mass
ΔV	Electrical polarization
E	Electric field
m_o	Electron mass
m_n	Electron effective mass
q	Electron charge
μ_n	Electron mobility
F	Force
n	Free electron concentration
E_F	Fermi level of semiconductor
p	Free hole concentration
m_p	Hole effective mass

μ_p	Hole mobility
θ_i	Hydrogen atoms coverage at the interface
n	Ideality factor
θ	Incident / Diffraction angle
c	Lattice constant
a	Lattice constant
B	Magnetic field strength
ϕ_M	Metal work function
n	Order of diffraction
h	Planck's constant
ε_r	Relative dielectric constant
A**	Richardson's constant
I_o	Saturation current
Φ_B	Schottky barrier height
χ	Semiconductor electron affinity
ϕ_S	Semiconductor work function
E_v	Valence band edge
V	Voltage
w	Width
W_C	Width of the pad
λ	Wavelength

LIST OF MAJOR ABBREVIATIONS

AFM	Atomic force microscope
NH_3	Ammonia gas
a.u.	Arbitrary unit
I-V	Current-Voltage
DC	Direct current
EDX	Energy Dispersive X-ray
FWHM	Full width at half maximum
HEMT	High Electron Mobility Transistor
HCl	Hydrochloric
HF	Hydrofluoric
HVPE	Hydride vapor phase epitaxy
LD	Laser Diode
LED	Light Emitting Diode
M	Metal
MESFET	Metal-Semiconductor FET
MIS	Metal-Insulator-Semiconductor
MOCVD	Metalorganic vapor deposition
MOSFET	Metal-Oxide-Semiconductor FET
MS	Metal Semiconductor
MSM	Metal Semiconductor Metal
MBE	Molecular Beam Epitaxial
PL	Photoluminscence
RF	Radio frequency

RHEED	Reflection high energy electron diffraction
RMS	Root mean square
SBH	Schottky barrier height
SEM	Scanning electron microscope
TE	Thermionic emission
TEM	Transmission electron microscopy
TEG	Triethylgallium
TMAl/TMA	Trimethylaluminum
TMGa/TMG	Trimethylgallium
TMIn/TMI	Trimethylindium
UHV	Ultra high vacuum
UV	Ultra Violet
VPE	Vapor Phase Epitaxy
XRD	X-ray Diffraction

PERTUMBUHAN RF-MBE STRUKTUR HETERO III-NITRIDA UNTUK APLIKASI PENGESANAN CAHAYA

ABSTRAK

Dalam penyelidikan ini, GaN p-n struktur homo, AlN/GaN struktur hetero, dan $Al_xGa_{1-x}N$/GaN struktur hetero telah berjaya ditumbuhkan di atas substrat silikon (Si) (111) menerusi epitaksi alur molekul plasma terbantu (MBE) untuk aplikasi pengesan foto. Galium (7N) dan aluminium (6N5) dengan ketulenan yang tinggi telah digunakan dalam sel Knudsen dan nitrogen (7N) berketulenan tinggi telah dibekalkan kepada frekuensi radio (RF) 13.56 MHz untuk menjana sumber spesis nitrogen reaktif. Nilai tekanan nitrogen dan kuasa pelepasan masing-masing ditetapkan malar pada $1.5x10^{-5}$ Torr dan 300 W sepanjang projek ini. Morfologi permukaan, sifat-sifat struktur dan optik daripada semua sampel telah disiasat dengan menggunakan pantulan belauan elektron bertenaga tinggi (RHEED), mikroskop imbasan elektron (SEM), mikroskop imbasan electron pancaran medan (FESEM), mikroskop electron transmisi (TEM), mikroskop daya atom (AFM), belauan sinar-X beresolusi tinggi (XRD-HR), fotoluminesen (PL), dan spektroskopi Raman, masing-masing. Untuk pertumbuhan GaN p-n struktur homo, Si dan magnesium (Mg) telah digunakan sebagai bahan dop n dan p, masing-masing. Imej-imej RHEED menunjukkan morfologi permukaan yang baik untuk lapisan GaN p-n struktur homo. Menurut imbasan ω / 2θ lengkung goyang simetri XRD satah (0002) pada suhu bilik, lebar sepenuhnya pada separuh maksimum (FWHM) untuk sampel GaN p-n struktur homo dikira sebagai 0.34^o, menunjukkan lapisan berkualiti baik bagi lapisan GaN. Kesan daripada fluk aluminium (Al) untuk kualiti kristal struktur hetero AlN/GaN pada substrat Si (111) telah dikaji. Ketebalan 69.94 nm (lapisan atas AlN) diperolehi

untuk keadaan pertumbuhan yang baik, memberikan FWHM daripada lengkung goyang XRD 0.46º (27.6 arcmin) setanding dengan sampel yang lain dan kerja-kerja sebelum ini. Didapati struktur hetero AlN/ GaN yang ditumbuhkan di bawah fluk Al yang rendah telah menghasilkan kualiti struktur yang baik dan nilai terikan mampatan yang rendah berbanding dengan sampel yang tumbuh di bawah fluk Al yang tinggi. Dua sampel dengan kandungan Al rendah iaitu struktur hetero $Al_{0.11}Ga_{0.89}N$ dan $Al_{0.29}Ga_{0.71}N$/GaN telah ditumbuhkan di atas substrat Si dengan FWHM daripada lengkung goyang XRD adalah masing-masing 0.62º dan 0.52º. Dengan menggunakan kaedah konvensional, nilai terikan bagi sampel struktur hetero $Al_{0.11}Ga_{0.89}N$ / GaN dan $Al_{0.29}Ga_{0.71}N$/GaN masing-masing dikira sebagai (+) 0.248% dan (-) 0.121%. Nilai-nilai ini adalah bersetuju dengan kajian oleh penyelidik lain. Penyiasatan sentuhan Pt yang disepuhlindap pada struktur hetero AlN/GaN pada pelbagai suhu penyepuhlindapan selama 10 minit dalam persekitaran nitrogen telah dilaksanakan dalam projek ini. Didapati bahawa ketinggian sawar Schottky (SBHs) dan permukaan sentuhan berubah dengan suhu penyepuhlindapan yang berbeza. Keputusan yang baik untuk SBH telah dicapai untuk sampel yang disepuh lindap pada 800ºC. Sementara itu, ciri-ciri sentuhan Ni/Ag yang disepuhlindapkan pada struktur hetero $Al_{0.11}Ga_{0.89}N$/GaN pada pelbagai suhu penyepuhlindapan selama 10 min dalam persekitaran oksigen juga dikaji dalam projek ini. Keputusan menunjukkan bahawa nilai SBH terbaik diperolehi untuk sampel Ni/Ag pada 700ºC. Pengesan foto GaN p-n struktur homo dan pengesan foto ultraungu (UV) logam-semikonduktor-logam (MSM) bagi sampel struktur hetero AlN/GaN dan $Al_xGa_{1-x}N$/GaN telah dibentangkan. Struktur hetero AlN/GaN dan struktur hetero $Al_xGa_{1-x}N$/GaN berasaskan MSM yang telah difabrikasikan untuk pengesan foto UV,

menandakan ciri-ciri konduktiviti foto yang baik, menunjukkan bahawa sampel mempunyai angkutan pembawa dan sifat kristal yang baik.

RF-MBE GROWTH OF III-NITRIDES HETEROSTRUCTURES FOR LIGHT DETECTING APPLICATIONS

ABSTRACT

In this research work, GaN p-n homostructures, AlN/GaN heterostructures, and $Al_xGa_{1-x}N$/Ga heterostructures were successfully grown on silicon (Si) (111) substrates by plasma-assisted molecular beam epitaxy (MBE) for photodetector applications. High purity gallium (7N) and aluminum (6N5) were used in the Knudsen cells and high purity nitrogen (7N) was supplied to 13.56 MHz radio frequency (RF) source to generate reactive nitrogen species. The nitrogen pressure and discharge power values were kept constant at $1.5x10^{-5}$ Torr and 300 W during this project, respectively. The surface morphology, structural and optical properties of all the samples were investigated by using reflection high energy electron diffraction (RHEED), scanning electron microscopy (SEM), field emission scanning electron microscopy (FESEM), transmission electron microscopy, atomic force microscopy (AFM), high-resolution X-ray diffraction (HR-XRD), photoluminescence (PL), and Raman spectroscopy, respectively. For the growth of GaN p-n homostructures, Si and magnesium (Mg) were used as n- and p-dopants, respectively. The RHEED images indicated a good surface morphology of GaN p-n homostructure layers. According to XRD symmetric rocking curve $\omega/2\Theta$ scans of (0002) plane at room temperature, the full width at half-maximum (FWHM) of GaN p-n homostructures sample was calculated as 0.34^o, indicating a good quality layer of GaN layer. The effect of the aluminum (Al) flux on the crystal quality of AlN/GaN heterostructures on Si (111) substrates was investigated. The thickness of 69.94 nm (AlN top layer) was obtained for good growth conditions giving the comparable

FWHM of the XRD rocking curve of 0.46° (27.6 arcmin) when compared with other samples and previous works. It was found that the AlN/GaN heterostructures grown under low Al-flux has produced a good structural quality and low compressive strain value compared to the samples grown under high Al-fluxes. Two samples of low Al-content $Al_{0.11}Ga_{0.89}N$/GaN and $Al_{0.29}Ga_{0.71}N$/GaN heterostructures were grown on Si substrates with FWHM of the XRD rocking curve of 0.62° and 0.52°, respectively. Using the conventional method, the strain values for samples$Al_{0.11}Ga_{0.89}N$/GaN and $Al_{0.29}Ga_{0.71}N$/GaN heterostructures were calculated as (+) 0.248 % and (-) 0.121 %, respectively. These values are in good agreement with the studies by other researchers. The investigation of annealed Pt contact on AlN/GaN heterostructures at various annealing temperature for 10 min in nitrogen ambient was conducted in this project. It was found that the Schottky barrier heights (SBHs) and surface of contact changed with different annealing temperatures. Good results for SBH have been achieved for sample annealed at 800°C. Meanwhile, the characteristics of annealed Ni/Ag contact on $Al_{0.11}Ga_{0.89}N$/GaN heterostructures at various annealing temperatures for 10 min in oxygen ambient were also studied in this project. The results revealed that the best SBH value was obtained for the 700°C annealed Ni/Ag contact on sample. GaN p-n homostructures photodetector and metal-semiconductor-metal (MSM) UV photodetectors of AlN/GaN and $Al_xGa_{1-x}N$/GaN heterostructures samples have been presented. The fabricated AlN/GaN heterostructures and $Al_xGa_{1-x}N$/GaN heterostructures based MSM for the UV photodetectors show good photoconductivity characteristics, suggesting that the samples have good carrier transport and crystalline properties.

.

CHAPTER 1

INTRODUCTION

1.1 Overview of III-Nitrides

III-Nitrides family (AlN, GaN, $Al_xGa_{1-x}N$, $In_xGa_{1-x}N$, etc.) are wide direct band gap semiconductor materials for optoelectronics, photonics applications, high power devices and high temperature electronics (Morkoc, 2003). These semiconductor materials have wide band gap energy starting from 3.33 eV to 6.2 eV, which covers from infra red wavelength to ultraviolet (UV) wavelength. In specific, III-nitride materials are great semiconductor materials for any optical or electrical device technologies such as surface acoustic wave (SAW) devices, UV photodetectors, light emitting diodes (LEDs) and laser diodes (LDs) for optical read and write applications (Morkoc, 2003). Nowadays, the applications of these III-nitride based LEDs can be found in electronic displays such as indicator lights, advertisement board, traffic signals and many more. High performance of digital read-write devices can be achieved by using III-nitride based short wavelength laser diodes. Moreover, the fuel efficiency in jet engines and automobiles can be improved by using III-nitride based UV photodetectors. The UV photodetector can also be used to control produced waste matters for a healthier environment (Morkoc, 2003).

Due to excellent properties such as high mobility, high breakdown voltage, high electron saturation velocity, high thermal conductivity, chemical inertness and mechanical stability, III-nitride semiconductor materials have become a popular choice in the fabrication of electronic devices capable of operating at high temperature, high frequency and high power densities (DeCuir *et al.,* 2008; Pearton *et al.,* 1999; Sze, 1990). III-nitrides with wurtzite structures are wide direct band gap

energy semiconductor. As shown in Figure 1.1, by tuning the composition of column III elements (lattice-mismatch issue needs to be considered in the material growth), the band gap energy of III-nitride semiconductor materials can cover the region from 0.7 eV (InN) to 6.2 eV (AlN). The direct and tunable band gap property makes III-nitride materials an excellent choice for optoelectronic devices including visible and UV light emitting diodes (LEDs).

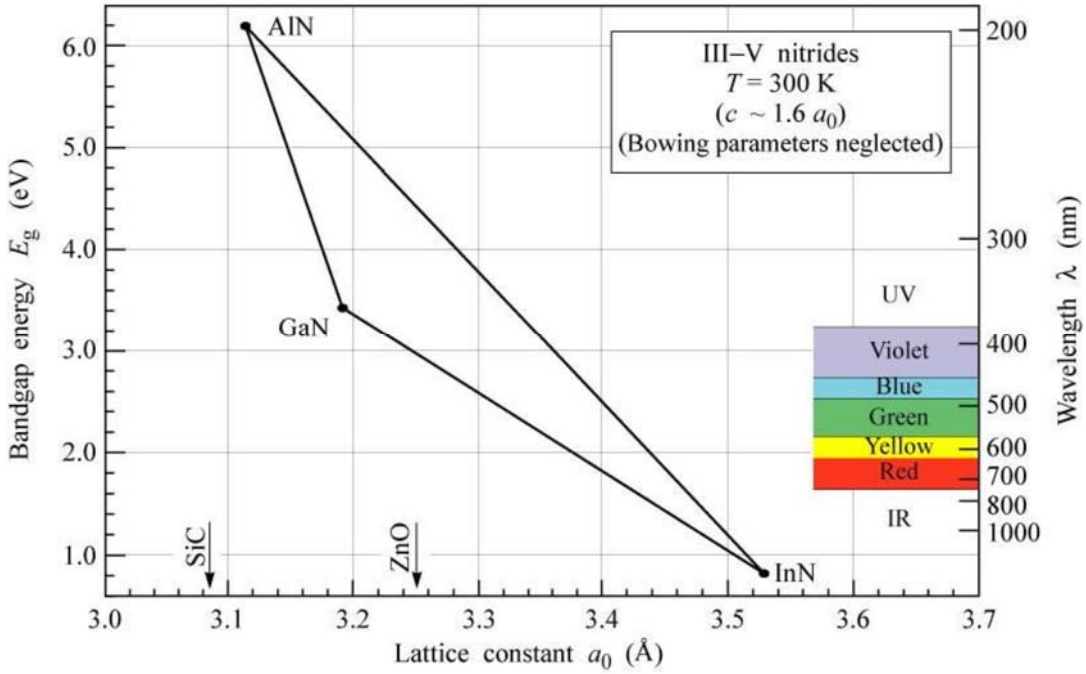

Figure 1.1: Bandgap energy versus lattice constant of III-nitride semiconductors at room temperature (adapted from Zhang, 2009).

GaN is normally observed as wurtzite 2H polytype (Figure 1.2 (a) and Figure 1.2 (b)) but it can also crystallize into a metastable zinc-blende 3C structure (Figure 1.3 (a) and Figure 1.3 (b)) (Mizuta *et al.,* 1986; Davis *et al.,* 1989; Petrov *et al.,* 1992; Strite *et al.,* 1993). However, another structure, which is rocksalt, or NaCl structure can also be induced in the GaN under very high pressures (Morkoc, 1999). There are two phases of crystalline for GaN, namely hexagonal symmetry and zinc-blende which are for wurtzite and cubic, respectively. The bandgap of hexagonal wurtzite

GaN is 3.4 eV and is one of most studied materials among all group III-nitrides. Maruska *et al.,* (1969) and Detcprohm *et al.,* (1992) reported that the lattice parameters of the wurtzite hexagonal GaN are: a = 3.1892 ± 0.0009 Å, and c = 5.1850 ± 0.0005 Å, respectively.

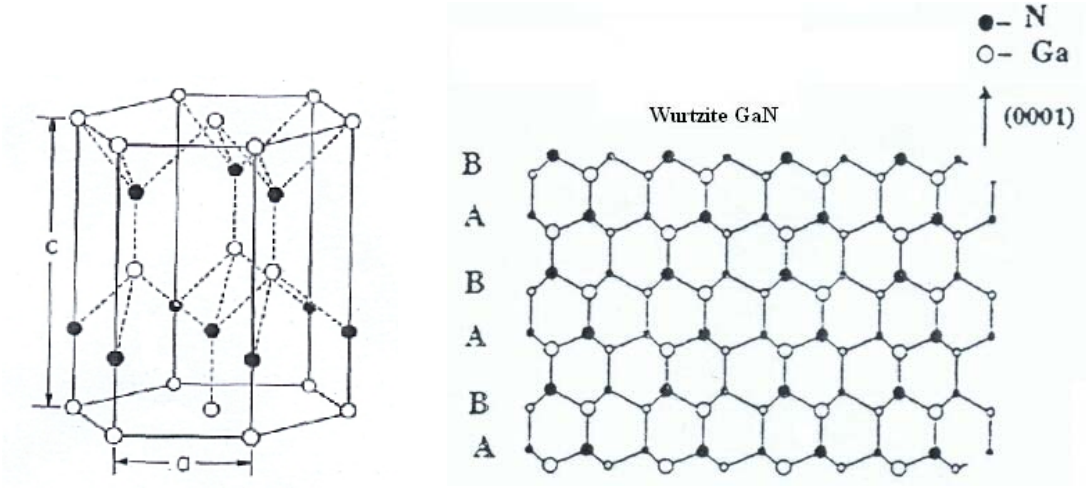

(a) (b)

Figure 1.2: (a)-(b) Wurtzite crystal structure of GaN (adapted from Morkoc *et al.,* 1994; Popovici & Morkoc, 2000).

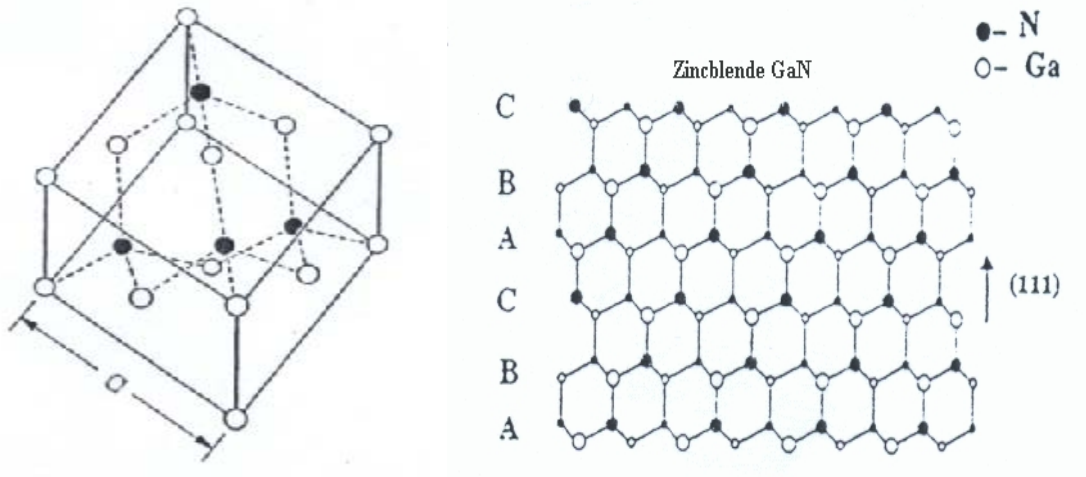

(a) (b)

Figure 1.3: (a)-(b) Zinc blende crystal structure of GaN (adapted from Morkoc *et al.,* 1994; Popovici & Morkoc, 2000)

1.2 Motivation for MBE Growth of III-Nitrides on Silicon Substrates

There are various methods to fabricate III-nitrides on Si substrates. Molecular beam epitaxy (MBE) is one of the most popular techniques used to grow high quality structures of the III-nitride alloy films. MBE can provide good uniformity and atomically sharp interfaces of heterostructure thin films. In this study, Mod Gen II plasma-assisted MBE is used to grow III-nitride materials on Si substrate. The Si substrates used in this research are of low cost, available in large diameters and have well characterized electrical and thermal properties. Si substrate reveals the great advantages of the well-known Si technology, low-cost production and potential hybrid integration with other device technologies (Pau *et al.,* 2002). The growth of a buffer layer by the plasma-assisted MBE in this work is one promising technique that can significantly reduce the structural defects and stress values at the Si/III-nitride alloy interface and it can also be used to electrically shield the thin films from the silicon substrate.

In previous studies, experimental researchers have successfully fabricated the III-nitride based photodetector, which can be utilized for flame detection, ultraviolet (UV) imaging or environmental monitoring (Muñoz *et al.,* 2001; Hirano *et al.,* 2001). The UV wavelength range has shown significant influence in optoelectronics research since the emergence of small and compact devices and high efficient light sources; eventually, new technologies are rising thanks to the integration of UV and visible detectors as well as light emitters and detectors. III-nitride based metal-semiconductor-metal (MSM) photodetector was also fabricated in this research and the electrical characteristics were analyzed using current-voltage (*I-V*) and photoconductivity measurements.

1.3 Problem Statements

III-nitride semiconductors are well-known in the fabrication of a number of optoelectronics and photonics technologies applications, but the problem regarding the growth processes still exists. The aims of this research work are to further the understanding of the basic growth process and the fabrication of a photodetector. The following problems are addressed:

1. One of the major challenges of fabricating high quality III-nitride thin films is the lack of a suitable substrate that is lattice-matched and thermally compatible with III-nitride heterostructure films. Si substrate is a popular substrate for growing III-nitride films due to its low cost and stability at high temperatures (Jain *et. al,* 2000). However, more cracks and dislocation densities are formed between III-nitride films and Si substrate because Si substrate has a large lattice-mismatch (about 17%) and a high thermal expansion coefficient mismatch. Therefore, an improved buffer layer (such as AlN) is needed to overcome the lattice-mismatch problem.
2. The nitrogen ratio and the growth temperature are the two parameters which are very important to achieve high crystalline III-nitride thin films (Jain *et al.,* 2000). Therefore, the nitrogen ratio and the growth temperature have to be optimized many times until the best growth condition for III-nitride thin films is achieved. Recently, the study on the effect of different nitrogen ratios and growth temperatures of III-nitride films on Si substrate is still progressing, pertaining to surface morphology, structural quality, strain properties and optical quality on the III-nitride thin films.

1.4 Research Objectives

1. The main objective of this work is to grow high quality III-nitride thin films on silicon substrate which include GaN p-n homostructures, AlN/GaN heterostructures and AlGaN/GaN heterostructures with various growth recipes, respectively.
2. The second objective is to study the effect of low and high temperatures AlN buffer layer on AlN/GaN heterostructures and AlGaN/GaN heterostructures, respectively.
3. The third objective is to investigate the effect of different nitrogen ratios and growth temperatures of AlN/GaN heterostructures and AlGaN/GaN heterostructures.
4. The fourth objective is to study the structural, optical and surface morphological qualities of GaN p-n homostructures, AlN/GaN heterostructures and AlGaN/GaN heterostructures on Si (111) substrates by using various measurement tools.
5. The fifth objective is to study the effect of thermal annealing on different metal-contact schemes (Ni and Ni/Ag contact schemes) on GaN p-n homostructures at various temperature conditions in nitrogen and oxygen ambient, respectively. Moreover, the effects of thermal annealing on Pt and Ni/Ag contacts on AlN and $Al_xGa_{1-x}N$ at various temperatures in nitrogen ambient are also carried out in this project, respectively.
6. Lastly, the development of GaN p-n homostructures, AlN and $Al_xGa_{1-x}N$ heterostructures for UV photodetectors also forms an objective of this thesis. The studies include both the effect of the material quality and metal-contact schemes on the UV detector performance.

1.5 Outline of the Thesis

In brief, the contents in this thesis are arranged as follows: The next **Chapter 2** will cover GaN-related matters and theories that are relevant to the work in this research. **Chapter 3** is devoted to the instrumentation employed in this research work. An explanation on the procedures and methods used, and some principles underlying the operation of the instruments are also covered. **Chapter 4** presents the studies of GaN p-n homostructure films from this research. The results of the fabricated photodetector with different metal contacts are also included in this chapter. In **Chapter 5**, the studies of AlN heterostructure films from this research are presented, analyzed and discussed. The results of AlN based photodetector are included in this chapter. Moreover, in **Chapter 6**, the investigation of $Al_xGa_{1-x}N$ heterostructure films from this research are presented, analyzed and discussed. The results of $Al_xGa_{1-x}N$ based photodetector are also included in this chapter. The final chapter, **Chapter 7**, concludes the thesis with a summary of the research work. Conclusion of the results obtained and some future work are also proposed in this thesis.

CHAPTER 2

LITERATURE REVIEW

2.1 Introduction

Fabrication of III-nitride semiconductors on Si substrates is useful from an industrial perspective as high crystalline quality and large size of Si substrate can be grown using low cost and effective methods (Matsuo *et al.,* 2007). Moreover, it is highly possible to integrate well-known Si technologies with III-nitride-based electronic and photonic devices on the same chip (Matsuo *et al.,* 2007). Until now, there have been more scientific research works on the growth of III-nitride semiconductor materials on Si substrate by researchers around the world. In this chapter, various growth methods of III-nitride semiconductors will be presented and described. The basic theories of metal-semiconductor contact are also discussed. Lastly, the general principle operation of photoconductor, p-n junction photodetector, and metal-semiconductor metal (MSM) photodetector will be described in the following subtopics.

2.2 Growth Technique of III-Nitrides Materials

III-nitride (GaN, AlN, InN, $Al_xGa_{1-x}N$, $In_xGa_{1-x}N$, etc.) semiconductor materials are normally deposited by chemical or physical vapor phase epitaxy (VPE) technique including hydride VPE (HVPE), metal-organic chemical vapor deposition (MOCVD), pulsed laser deposition (PLD), molecular beam epitaxy (MBE) and many more. HVPE, MOCVD and MBE are the more famous methods compared to the other methods.

2.2.1 Hydride Vapor Phase Epitaxy (HVPE)

The HVPE method can fabricate III-nitride semiconductors of good crystal structure, optical and electronic quality. The HVPE offers high growth rate and large diameter wafer can be transferred into HVPE system (Kirilyuk *et al.,* 2001). Furthermore, it is a low-cost method compared to other method. Due to these advantages, the HVPE method is a popular choice for industry to fabricate large GaN substrates (Hagemen *et al,* 2003). In the HVPE process, group III-nitrides are grown on substrate by reacting hot gaseous metal chlorides (e.g., GaCl or AlCl) with ammonia gas (NH_3). The metal chlorides are produced by flowing hot HCl gas over the hot group III metals. All reactions are done in a temperature controlled quartz furnace.

$$HCl\ (g) + Ga(l) \longrightarrow GaCl\ (g) + \frac{1}{2}H_2(g)$$

$$GaCl(g) + NH_3(g) \longrightarrow GaN(s) + HCl\ (g) + H_2\ (g)$$

2.2.2 Metal-Organic Chemical Vapor Deposition (MOCVD)

MOCVD is a chemical vapor deposition method used to grow high quality, single or polycrystalline thin layers of semiconductors. This method is a popular choice for industrial companies to fabricate a number of high performance optoelectronics and high speed electronic devices. Trimethylgallium (TMG) and triethylgallium (TEG) are normally used for Ga element, while GaCl has sometimes been used to provide Ga (Morkoc, 1999). Trimethylindium (TMI) and trimethylaluminium (TMA) are generally used for In and Al elements, respectively (Morkoc, 1999). Ammonia (NH_3), the source used for chemical vapor deposition is considered a popular source of nitrogen as it is a pure and stable gas in nature (Morkoc, 1999).

Hydrogen carrier gas is used to transfer precursors into the growth chamber and then precursors are introduced into reaction chamber. The gas manifold allows the separate injection of ammonia (Morkoc, 1999). Figure 2.1 is a schematic diagram of MOCVD system. Sapphire substrate with C-plane (0001) orientation is popularly used as a foreign substrate for III-nitride growth (Morkoc, 1999). In the MOCVD reactor, TMG, TMA, or TMI reacts with ammonia on the substrate, which is heated to about 1000^{o}C where the common feature here is that all the reaction processes between group III elements, dopants and precursors must occurred on the substrate surface only (Morkoc, 1999).

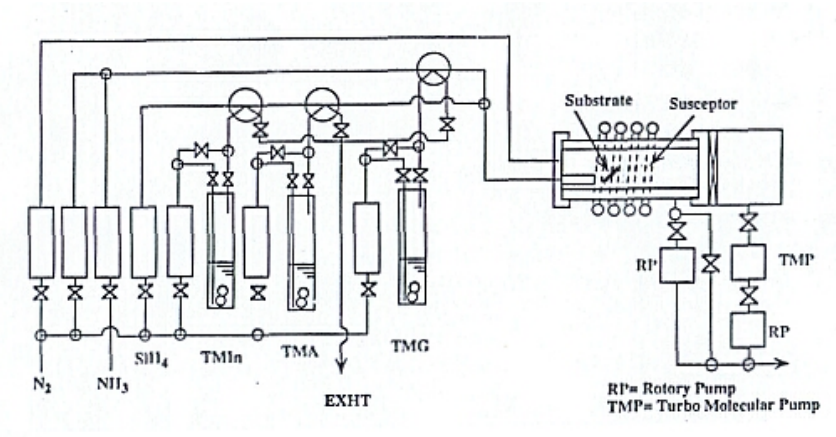

Figure 2.1: Diagram of a horizontal MOCVD reactor (adapted from Akasaki, I, Meijo University).

2.2.3 Molecular Beam Epitaxy (MBE)

Molecular Beam Epitaxy (MBE) was developed during the 1970s for the growth of III-V semiconducting compounds and rapidly became established as a tremendous technique for producing thin films of high purity and well defined thickness for a wide variety of device structures. It came particularly into its own in the 1980s with the development of low dimensional structures, which required atomic layer precision in the deposition of multi-layers; the classic examples being those of AlGaAs/GaAs quantum well, superlattice and two-dimensional electron gas

structures. MBE is characterized by growth under ultra-high vacuum conditions and a readily available in situ monitoring method in the form of reflection high energy diffraction (RHEED).

2.3 Influential Parameters on III-Nitride Group

The quality of III-nitride materials grown on the substrates by plasma-assisted MBE is determined by several factors. Among the important factors are the types of substrate and buffer layers.

2.3.1 Substrates

Generally, III-nitride semiconductor based devices are fabricated on sapphire (Al_2O_3) or silicon carbide (SiC) substrates. However, these substrates are very expensive and sapphire is an insulator in nature. Moreover, these substrates are also large diameter substrates. Moreover, Monemar *et al.,* (1997) reported that the biaxial strains and compressive are occurred when GaN deposited on sapphire or 6H-SiC substrate. However, the strain in the GaN film can be released with the assist of threading dislocations formation. The direct growth of GaN on 6H-SiC has a hexagonal crystal structure without any buffer layer. The growth of GaN on 6H-SiC offer high thermal and electrical conductivity, respectively, however, this substrate is very expensive (Honda *et al.,* 2000).

Si substrate is the suitable candidate for the III-nitride growth, due to low cost and is a conducting substrate compared with the others. III-nitride based electronics and optoelectronics can be integrated with well-known Si based electronics. Moreover, optical, structural, thermal and electronic properties Si are well investigated. However, the presence of cracking on the III-nitride layers due to stress

makes the Si substrate not a famous selection for high quality growth of III-nitride layers. Moreover, the presence of stress values is not very high for III-nitrides on sapphire or III-nitrides on SiC substrates. In 1998, the first GaN LED on Si substrate was reported by Guha and Bojarzuk (1998a) and (1998b). They had successfully grown p-type GaN on Si substrate. There is nearly 16% of lattice mismatch between silicon substrate and GaN layer, which produces high dislocation density in the GaN layers. Moreover, thermal mismatch is almost 54% that causes a major problem for the device operation. Therefore, it is very hard to produce thick GaN layers without cracks and defects. Another advantage of using Si substrate is the resistivity of Si can reach up to 10^4 ohm-cm which is lower than the resistivity value of sapphire, SiC or GaN. According to Chuah *et al.* (2009a), X-ray diffraction (XRD) pattern showed that the full width at half maximum (FWHM) of AlN (0002) peak grown on Si (111) substrates was smaller than that grown on Si (100) substrates. The AlN films grown on Si (111) substrate has a good preferred orientation and it is easy to control compared to AlN on Si (100). Moreover, Si (111) substrate offers only 19 % lattice mismatch for AlN thin films. The structure of AlN and Si (111) are both hexagonal structures. However, an AlN film grown on Si (100) substrate has a larger lattice mismatch (42.7%) and larger strain value. This is because Si (100) substrate has a square lattice, therefore unmatched with hexagonal AlN film. Meanwhile, for GaN film grown on AlN buffer layer, the crystal structure quality of GaN is improved due to lower lattice mismatch percentage (2.5%) between GaN and AlN buffer layer.

2.3.2 Buffer Layer

It is known that III-nitrides materials on silicon substrate normally have lower quality compared to materials grown on other substrates like sapphire or SiC

(Schremer *et al.,* 2000). In fact, the III-nitrides and Si substrate are not in the same crystal system and have major differences in their thermal expansion coefficients. Using conventional two-step method, the fabrication of gallium nitride on silicon substrate has resulted in a very poor surface morphology and crystal quality of the grown layers. For conventional two-step method, the GaN epilayers are grown on top of a thin AlN buffer/nucleation layer (Lu *et al.,* 2002). Therefore, it is challenging to produce good uniformity and crystalline quality of GaN layer on silicon substrate. Previously, there are many types of buffer layers such as 3C-SiC (Takeuchi *et al.,* 1991), AlN (Kung *et al.,* 1995; Lu *et al.,* 2002), GaAs (Yang *et al.,* 1996), AlAs (Strittmatter *et al.,* 2000), Si_3N_4 (Nakada *et al.,*1998) and γ-Al_2O_3 (Wang *et al.,* 1998) that have been employed as the buffer layer between the GaN layer and the Si substrate.

The quality of GaN epitaxial layer has been found to be very sensitive to the initial surface coating on Si substrates and is being improved by exploring the AlN buffer layer between GaN and Si substrate (Davis *et al.,* 2001; Hiroyama and Tamura, 1998; Chen *et al.,* 2001). AlN (0001) (a=3.112Å) is the most popular and successful buffer material because of its superior thermal stability, 5:4 magic lattice matching with Si (111). A 5:4 magic lattice is referring to the coincidence lattice between AlN and the silicon substrate (Schenk *et al.,* 1999c). This is because the lattice and thermal mismatch between AlN and GaN are much smaller than those between Si and GaN, and AlN has good wetting properties on Si (Chen *et al.,* 2001). The latter changes the tensile strain (~mismatch: +17%) to compressive (~mismatch: -2.47%) for later GaN growth. AlN buffer is often used together with other methods, such as the intentional nitridation or epitaxial lateral overgrowth (ELO) methods. Of all the revised strategies, two kinds of aluminum-assisted AlN buffer should be

specially noted. Sánchez *et al.,* (2002) reported the effect of AlN buffer layer thickness on the crystal quality of GaN/AlN/Si(111) heterostructures grown by plasma-assisted molecular beam epitaxy (PA-MBE). They found that smaller buffer layer thickness leads to higher inversion domains density reaching the GaN surface (Sánchez *et al.,* 2002). As can be seen in Figure 2.2, by using AlN buffer layer, better uniformity and high quality for thin films layers have been successfully fabricated on the silicon substrate (Hussien *et al.,* 2009). In this case, AlN buffer layer is commonly used to grow high crystalline quality of AlGaN/GaN heterostructures and it also used to electrically shield the AlGaN/GaN heterostructures from the conducting silicon substrate (Pau *et al.,* 2002). Moreover, the AlN buffer layer reduces the defects, lattice mismatch and biaxial strain in the AlGaN/GaN heterostructures (Tansley *et al.,* 1997).

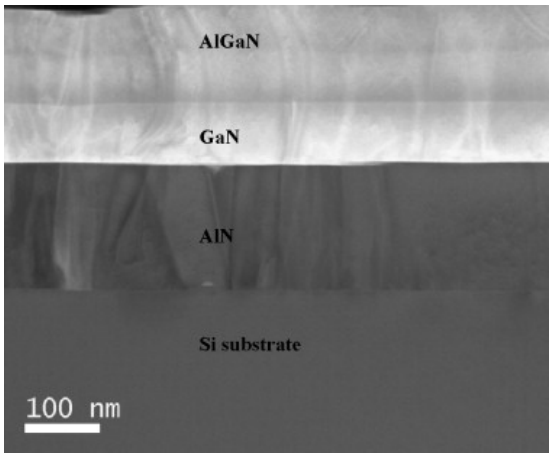

Figure 2.2: Cross-sectional TEM image of $Al_xGa_{1-x}N$/GaN/AlN film grown on the Si(111) substrate (adapted from Hussien *et al.,* 2009).

2.4 Growth of GaN P-N Homostructures

The p-n junctions are of great importance both in modern electronics applications and in understanding other semiconductor devices. The p-n junction theory serves as the foundation for the physics and semiconductor characteristics of p-n junction; it

was established by Shockley (1949). This theory was then extended by Sah *et al.* (1957) and Moll (1958). Devices such as p-i-n photodiodes have demonstrated the potential to respond to the requirements for the future since the progress made in the improvement of quality of GaN epilayers has been remarkable. The first information about p-n GaN photodiodes had been reported by Khan *et al.,* (1995) and Chen *et al.,* (1995). Alias *et al.,* (2015) presented the properties of GaN p-n junction grown on A Si substrate by molecular beam epitaxy (MBE) at different annealing temperature. They revealed that thermal treatment via a resistance furnace has improved the properties of the GaN p-n junction grown on a Si substrate up to 1,000ºC. However, the electrical characteristics of the sample were degraded due to the diffusion of Si atom toward the p-GaN layer. One of the key technologies used in the fabrication of those devices is the developed low defect density intrinsic layer, high quality p-type material and thus improves the insulating layer as had been reported by Pernot *et al.,* (1998). The leakage current in a GaN p-n homostructures is theoretically very low; however a previous publication reported a relatively large leakage current, which reduced the possibility of low UV light detection, especially under temperature fields (Osinsky *et al.,* 1997). Different groups proposed that one of the causes of the leakage current is the reactive ion etching (RIE)-induced damages at the mesa sidewalls (Van Hove *et al.,* 1997). Tunneling effects appear to be the main reason for junction breakdown, and the main reason for the difference between the theoretical and measured dark current value under low reverse bias voltage is suggested to be the surface leakage along sidewalls (Pernot *et al.,* 1998). Kozodoy *et al.,* (1998) used lateral epitaxial overgrowth (LEO) to remove threading dislocations in GaN p-n junction. They found that the leakage current magnitude without threading dislocation is reduced more than 3 orders compared to the sample with threading

dislocation. Cao *et al.*, (1999) presented the growth of n^+-p junction in GaN by the implantation of $^{29}Si^+$. They found that the ideality factor n and the breakdown voltage were calculated as ~2 and 13 V, respectively.

2.4.1 The Performance of GaN P-N Photodetectors

Recently, Vikas *et al.,* (2016) showed the fabrication of n-ZnO/p-GaN heterojunction over Mg:GaN substrate by hydrothermal method. The heterojunction device revealed excellent rectification behavior with a rectification ratio of 5.4 at 3V. Moreover, the device also showed selective UV response and good response to UV light pulses. Nakagomi *et al.,* (2015) prepared β-Ga_2O_3 thin film on p-type GaN template substrates. The β-Ga_2O_3/p-GaN photodiode showed good rectifying properties. The responsivity of the device was highest under deep-UV light below a wavelength of 240 nm. Meanwhile, Yakuphanoglu *et al.,* (2015) presented a new type of photodiode, p-Si/GaN pn junction in series with GaN/Ag Schottky diode. They used facile sol gel method to synthesize nanostructures GaN nanorods. The diode current of Al/p-Si/GaN/Ag diode (dark current= $4.80x10^{-6}$ A) increases to $4.12x10^{-5}$, $6.81x10^{-5}$, $1.03x10^{-4}$ and $1.42x10^{-4}$ A after illuminating the device with light intensity of 30, 60, 80, and 100 mW/cm^2, respectively. Tuan *et al.,* (2015) reported the fabrication of p-n GaN diodes by using the magnetron sputtering. The leakage current, turn-on voltage, ideality factor, and breakdown voltage of the GaN p-n photodetector device were found to be 2.2 $x10^{-7}$ A, 2.2 V, 5.0, and -6 V, respectively, at room temperature. Bao *et al.,* (2013) fabricated a planar GaN based p-i-n photodetector by Si implantation into GaN based p-i-n structure grown by metal-organic chemical vapor deposition (MOCVD). The dark current density and

responsivity of the device are measured as 1.03 nA/cm^2 and 0.122 A/W at 360 nm, respectively.

2.5 Growth of AlN/GaN Heterostructures

In principle, AlN is the most interesting candidate for future high-power devices, high-temperature microelectronics and deep-UV optoelectronics applications since it possesses a band gap of 6.2 eV at room temperature, a melting temperature greater than 2700^{o}C and a thermal conductivity of 3.2 W cm^{-1} K^{-1} (Rivera-Julio *et al.,* 2013; Strite and Morkoc, 1992). However, to realize the full potential of AlN, device-quality materials must be developed with controllable n-type and p-type doping. AlN has also been reported to have negative electron affinity (Benjamin *et al.,* 1994) and is therefore a promising candidate for low-voltage field emission devices. It is also of interest as a substrate for GaN-based devices because of its similar lattice constant (~1% mismatch) and thermal expansion coefficients.

In recent years, many groups have focused on GaN growth on Si substrate. This is mainly due to the advantage of being low cost and having large sized Si wafer as substrate and also the potential to integrate GaN high power electronics and light emitting diodes (LEDs) with the highly matured Si technology. However, the large lattice mismatch and strong Si-N bond make it difficult to achieve high quality GaN epilayer on Si directly. Due to the good wetting characteristic between Al and Si surface, it is easier for the AlN growth on Si than that of GaN.

Good quality of III-nitrides can be achieved using AlN buffer layer (Adikimenakis *et al.,* 2009) and (Ajagunna *et al.,* 2009). Unfortunately, the fabrication and characterization of aluminum nitride itself are still ongoing process (Le Louarn *et al.,* 2009; Yamabe *et al.,* 2009). Hu *et al.,* (2011) reported that the

lower FWHM of AlN on silicon substrate was achieved when the sample was fabricated at high temperature. The transmission electron microscopy (TEM) study by Kaiser *et al.,* (1999) is concerned with the microstructure of AlN grown via MBE on Si (111). They studied the defect types as a function of substrate temperature during growth between 700ºC and 800ºC and Al/N-flux ratios of about 1 up to large Al excesses. The AlN layers were grown on Si (111) with high (optimum) quality according to the X-ray diffraction. Chuah *et al.,* (2009) reported the growth of AlN cap layer on GaN grown on Si (111) substrate via PA-MBE. They presented the FWHM of AlN peak as 26 arcmin, which is comparable with the reported values by Dadgar *et al.,* (2006).

2.5.1 The Performance of AlN Photodetectors

Tsai *et al.,* (2013) presented the AlN based metal-semiconductor-metal (MSM) photodetector grown on p-type Si by using a reactive sputtering method. The MSM device revealed a dark current as low as ~ 1 nA at a bias up to 200 V. Moreover, the response times and recovery times of the device were recorded as fast as ~ 110 ms and 80 ms, respectively. Meanwhile, Barkad *et al.,* (2010) reported the fabrication and characterization of solar-AlN based blind deep ultraviolet (DUV) MSM photodetectors. For the device contact, the TiN was used as a Schottky contact. The DUV MSM device presented a very low dark current of 100 fA at $\pm$ 100V DC. Moreover, their device also showed a high sensitivity to DUV light and a sharp cut-off wavelength around 203 nm, close to the band gap of bulk AlN.

Chuah *et al.,* (2009a) reported the fabrication of AlN/GaN heterostructures on silicon substrate for Schottky photodetector applications. The best Schottky contact is obtained for the 700ºC annealed sample. The contrast ratio for the 700ºC annealed

sample and control Schottky diode was found to be 25 and 2, respectively. BenMoussa *et al.,* (2008) demonstrated the suitability of the AlN MSM photodiode for vacuum ultraviolet (VUV) applications. The MSM device showed a negligibly small dark current of 13 fA at -30V. The measured responsivity curves at $\pm$30V show the AlN band edge to be around 203 nm and show a rejection ratio 200/300 nm of more than four orders of magnitude. Yu *et al.,* (2006) showed the novel characteristics of the AlN/GaN heterostuctures based UV Schottky barrier photodetectors. The leakage current for the device was shown to be about four orders of magnitude smaller than for the conventional Schottky barrier photodetectors. The responsivity and UV to visible rejection ratio are recorded as 0.16 A/W and 7.74 $x10^2$ under -5 V applied bias, respectively.

2.6 Growth of $Al_xGa_{1-x}N$/GaN Heterostructures

$Al_xGa_{1-x}N$ alloys are very important materials with extensive applications for electronics and optoelectronic semiconductor devices because these materials have a direct wide band gap, which ranges from 3.4 to 6.2 eV. These materials are very famous materials for applications in ultraviolet (UV) laser diodes (LDs), light emitting diodes (LEDs) and photodetectors. By far the most published interest in $Al_xGa_{1-x}N$-based devices has been for HEMTs, with the first published observation of an $Al_xGa_{1-x}N$ HEMT was done by Khan *et al.,* (1994). The mole fraction is controlled by the: 1) Al flux, 2) Ga flux, 3) both Ga and Al fluxes with a fixed Al/Ga ratio and 4) Al/Ga ratio with a fixed total flux (Yun, 2006). As for GaN, Ga-rich growth conditions are preferred to obtain high quality films. However, the growth of $Al_xGa_{1-x}N$ under Ga-rich conditions via plasma-assisted MBE received little attention since the precise control of the Al mole fraction, *x* is difficult.

2.6.1 The Methods Use to Determine The Al composition in The $Al_xGa_{1-x}N$ Layer

There are many methods exist for the measurement of Al mole fraction in $Al_xGa_{1-x}N$ layers including x-ray diffraction (XRD), photoluminescence (PL), X-ray photoemission spectroscopy (XPS) and Raman spectroscopy. Table 2.1 shows summary of the methods used to determine the Al composition in the $Al_xGa_{1-x}N$ layer. The following subtopic is a brief discussion of the different methods use to calculate Al mole fraction in $Al_xGa_{1-x}N$ layers.

Table 2.1: Summary of the common methods used to determine the Al composition in the $Al_xGa_{1-x}N$ layer.

Growth Methods of $Al_xGa_{1-x}N$	Al Determination Methods	Al composition in $Al_xGa_{1-x}N$	References
Plasma assisted MBE	XRD	~0.1	Novikov *et al.*, 2015
MOCVD	XRD Optical Transmission	0.28	Wang *et al.*, 2015
Hollow cathode plasma-assisted atomic layer deposition	XRD, XPS	0.68, 0.95, 0.96	Goldenberg *et al.*, 2014
MOCVD	Raman	0.48	Gao *et al.*, 2013
LPMOCVD	XRD, PL	x<0.14	Dang-Hui *et al.*, 2013
HVPE	XRD	0.45	Hagedorn *et al.*, 2012
HVPE	UV-Vis, spectrophotometry XRD, XPS	0.23, 0.26, 0.27	Lee *et al.*, 2012
Pulsed Atomic Layer Epitaxy	XRD	0.91	Pan *et al.*, 2011
RF-MBE	XRD	0.07-0.1	Kakuda *et al.*, 2011
RF-MBE	XRD	0.24, 0.25	Hussien *et al.*, 2011a
RF-MBE	XRD	0.11, 0.24, 0.30, 0.43	Hussien *et al.*, 2011b
-	XRD, PL	0.29	Young *et al.*, 2011
MOCVD	XRD, PL, XPS	x<0.25	Bahn *et al.*, 2003

2.6.1(a) HR-XRD

High resolution XRD is a powerful tool to precisely determine the lattice constants of thin crystal films. Moreover, this tool is also widely used to determine the Al composition in the $Al_xGa_{1-x}N$ films. Using the Bragg equation, the lattice constant c_{epi} of AlGaN can be accurately calculated. Figure 2.3 shows the skew symmetric 2θ/ω scan of (1015) diffraction of AlGaN/GaN heterostructures.

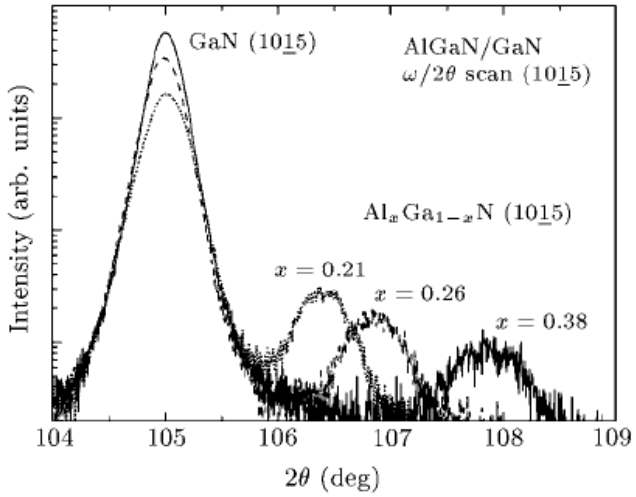

Figure 2.3: X-ray 2θ/ω scan of the (1015) diffraction from AlGaN/GaN heterostructures with different Al compositons (adapted from Sheng-Qiang *et al.*, 2005).

For the full relaxed alloy, the chemical composition can be calculated simultaneously from the lattice constants according to Vegard's law that is assumed to be linear for semiconductor alloy system. Using Vegard's law, the Al composition is calculated from lattice constant a and c, respectively, by the following equations:

$$a(x) = a_o^{GaN}(1-x) + a_o^{AlN}x \tag{2.1}$$

$$c(x) = c_o^{GaN}(1-x) + c_o^{AlN}x \tag{2.2}$$

where $a_o^{GaN} = 0.3189\,nm$, $c_o^{GaN} = 0.5185\,nm$, $a_o^{AlN} = 0.311\,nm$, and $c_o^{GaN} = 0.498\,nm$ were the relaxed lattice constant for GaN and AlN, respectively.

Meanwhile, the Al compositions of the $Al_xGa_{1-x}N$ samples can also be evaluated through the XRD measurements where XRD symmetric rocking curve (RC) ω scans of (0002) $Al_xGa_{1-x}N$ epilayer is recorded (Hussien *et al.*, 2011a, 2011b). The full width at half-maximum (FWHM) of the rocking curve for the $Al_xGa_{1-x}N$ peaks are firstly calculated. From the XRD symmetric RC ω scans and application of Vegard's law, the Al composition in the $Al_xGa_{1-x}N$ films can be determined. Figure 2.4 shows the XRD rocking curve of (0002) plane of $Al_xGa_{1-x}N$/GaN/AlN grown on Si(111) substrate (Hussien *et al.*, 2011a).

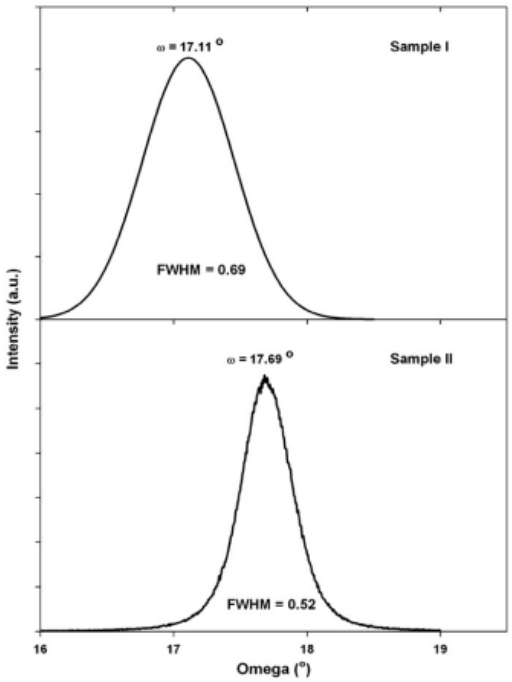

Figure 2.4: XRD rocking curve (RC) of (0002) plane of $Al_xGa_{1-x}N$/GaN/AlN grown on Si(111) substrate for samples I and II (adapted from Hussien *et al.*, 2011a).

2.6.1(b) Photoluminescence

Photoluminescence is a suitable tool to determine the $Al_xGa_{1-x}N$ band gap and Al composition in $Al_xGa_{1-x}N$ layer. The photon energy of excitation light source is much

larger than band gap of the $Al_xGa_{1-x}N$ layer. A He-Cd laser, with a photon energy of 3.81 eV, can be used as an excitation light source for the measurement of Al content in $Al_xGa_{1-x}N$ alloys with Al mole fraction x up to ~15 percent. However, for $Al_xGa_{1-x}N$ layers with x > 0.15, the photon energy from this laser is too low and a different source is required. For example, a He-Cd laser (325 nm) and Xe lamp with band-pass filter (400 nm) were used as excitation sources in photoluminescence characterization of Eu and Mg codoped $Al_{0.11}Ga_{0.89}N$ on GaN template (Kanemoto *et al.,* 2015). Figure 2.5 presents PL spectra of AlGaN/GaN epilayers with Al compositions measured at room temperature. The excitation wavelength used in this work is 244 nm. The high intensity at 3.4 eV peak is found to represent near band-edge emission of GaN. As expected, $Al_xGa_{1-x}N$ peak related to the band-edge transitions is found to show a blue shift with increasing Al solid reaction (Jayaskathi *et al.,* 2014).

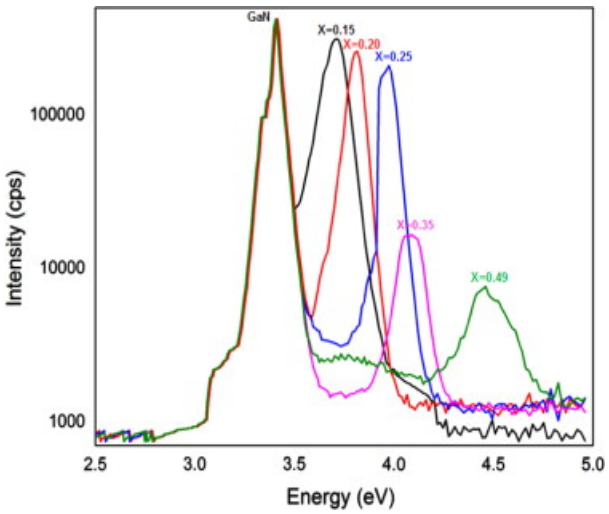

Figure 2.5: Room temperature PL spectra of AlGaN/GaN for different composition of Al (adapted from Jayaskathi *et al.,* 2014).

The mole fraction of Al has been determined by compositional dependence of the optical band gap of ternary alloys using the following equation (Dang-Hui *et al.,* 2013).

$$E_{g,AlGaN}(x) = xE_{g,AlN} + (1-x)E_{g,GaN} - bx(1-x) \quad (2.3)$$

Where E_g, x and b are the optical band gap, AlN mole fraction and bowing parameter, respectively. E_{gGaN}, E_{gAlN} and b are 3.43 eV, 6.05 eV and 0.9 eV, respectively (Vurgaftman and Meyer, 2007). The bowing parameter values reported in the literature are in the range of 0.8-2.6 eV (Lee *et al,* 1999). The AlGaN emission and Al composition determined from PL spectra are reported in Table 2.2 below.

Table 2.2: PL emission of AlGaN layers (adapted from Jayaskathi *et al.,* 2014).

Sample no	PL emission wavelength (nm)	Al composition x
I	335	0.15
II	325	0.20
III	316	0.25
IV	300	0.35
V	277	0.49

2.6.1(c) XPS

X-ray photoemission spectroscopy (XPS) is normally used to analyze the surface chemistry of a material. It also can be used to determine the elemental composition, empirical formula, chemical state and electronic state of a material. For the ternary compound sample, XPS is used to determine the Al composition in the $Al_xGa_{1-x}N$ film. Figure 2.6 is the fine spectra for the Al2p and $Ga2P_{3/2}$ states taken in the narrow-scan mode. The Al mole fraction is determined from the relative ratio of the integrated peak intensity of Al2p to that of $Ga2P_{3/2}$ for each spectrum. Here, the values of 0.193 and 3.34 were used as the reference sensitivity factors (RSFs) for the Al2p and $Ga2P_{3/2}$ states, respectively (Bahn *et al.* (2003).